Meteoritics & Planetary Science 37, 75–89 (2002)
Available online at http://www.uark.edu/meteor

A critical evaluation of oxidation *versus* reduction during metamorphism of L and LL group chondrites, and implications for asteroid spectroscopy

HEATHER K. GASTINEAU-LYONS[1], HARRY Y. MCSWEEN, JR.[1]* AND MICHAEL J. GAFFEY[2]

[1]Department of Geological Sciences, University of Tennessee, Knoxville, Tennessee 37996, USA
[2]Department of Space Studies, University of North Dakota, Grand Forks, North Dakota 58202, USA
*Correspondence author's e-mail address: mcsween@utk.edu

(Received 2000 December 7; accepted in revised form 2001 October 3)

Abstract–Modal mineralogies of individual, equilibrated (petrologic type 4–6) L and LL chondrites have been measured using an electron microprobe mapping technique, and the chemical compositions of coexisting silicate minerals have been analyzed. Progressive changes in the relative abundances and in the molar Fe/Mn and Fe/Mg ratios of olivine, low-Ca pyroxene, and diopside occur with increasing metamorphic grade. Variations in olivine/low-Ca pyroxene ratios (Ol/Px) and in metal abundances and compositions with petrologic type support the hypothesis that oxidation of metallic iron accompanied thermal metamorphism in ordinary chondrites. Modal Ol/Px ratios are systematically lower than normative Ol/Px ratios for the same meteorites, suggesting that the commonly used C.I.P.W. norm calculation procedure may not adequately estimate silicate mineral abundances in reduced chondrites. Ol/Px ratios calculated from visible and near-infrared (VISNIR) reflectance spectra of the same meteorites are not in agreement with other Ol/Px determinations, possibly because of spectral complexities arising from other minerals in chondrites. Characteristic features in VISNIR spectra are sensitive to the proportions and compositions of olivine and pyroxenes, the minerals most affected by oxidative metamorphism. This work may allow spectral calibration for the determination of mineralogy and petrologic type, and thus may be useful for spectroscopic studies of asteroids.

INTRODUCTION

Parent bodies of the ordinary chondrites were thermally metamorphosed soon after their accretion. Mineralogic variations among chondrites of different metamorphic grade (petrologic type) have been previously attributed to either oxidation (McSween and Labotka, 1993) or reduction (Dodd, 1976; Brett and Sato, 1984; Sears and Weeks, 1986) reactions during metamorphism. Verification of changes in oxidation state has important implications for understanding metamorphic conditions and fluid–rock interactions in chondritic asteroids otherwise thought to have been dry. A practical application of this study derives from recognition that the relative abundances and chemical compositions of olivine and pyroxenes, the phases most affected by redox reactions in ordinary chondrites, control their visible and near-infrared (VISNIR) reflectance spectra. Determining the proportions of these minerals is thus important for the calibration of asteroid spectra.

Here we evaluate evidence for oxidation *vs.* reduction in metamorphosed L and LL chondrites. The selection of these chondrite groups was originally motivated by the *Near-Earth Asteroid Rendezvous–Shoemaker (NEAR)* spacecraft encounter with asteroid 433 Eros, which has spectral reflectance similar to L and LL chondrites (Bell *et al.*, 2000; Veverka *et al.*, 2000). Our choice of meteorites to be studied was also influenced by the spectral survey of Gaffey (1998), who concluded that terrestrial weathering had affected most ordinary chondrites. He identified a small subset of "spectrally clean" chondrites which are most appropriate for comparison with asteroid spectra. Most of the chondrites studied here are spectrally clean.

McSween and Labotka (1993) suggested that the following oxidation reaction, caused by small amounts of aqueous fluid, occurred during metamorphism of H, L, and LL chondrites:

$$\underset{\text{metal}}{Fe} + O_2 + \underset{\text{low-Ca pyroxene}}{(Mg,Fe)SiO_3} \Rightarrow \underset{\text{olivine}}{(Mg,Fe)_2SiO_4}$$

This reaction would have produced changes in the relative proportions of olivine, low-Ca pyroxene, and metal with increasing petrologic type. Mineral abundances in ordinary chondrites were estimated (McSween *et al.*, 1991) by calculating mineral norms from the bulk chemistry of 94 unweathered falls in which metallic Fe and FeS had been measured. The C.I.P.W. norm calculation is a standard petrologic tool that recasts bulk-rock chemistry into a set of idealized minerals; the resulting *normative* mineral proportions may

Prelude preprint MS#4478

differ from the actual minerals present (the *modal* abundances). Norm calculations for ordinary chondrites indicate that the average ratio of olivine to low-Ca pyroxene (henceforth called Ol/Px) increases with petrologic type, as the proportion of metal decreases (McSween and Labotka, 1993), consistent with the oxidation hypothesis.

If some metallic iron were oxidized, the residual metal should contain higher concentrations of Ni and Co. Rubin (1990) noted that Ni/Fe and Co/Fe in kamacite increase with petrologic type in H, L, and LL chondrites, and McSween and Labotka (1993) observed the same trends in the bulk chondrite metal analyses of Jarosewich (1990). McSween and Labotka (1993) also observed that average olivine and low-Ca pyroxene compositions in H, L, and LL chondrites have higher Fe/Mg with increasing petrologic type, suggesting that some Fe^{2+} formed by metal oxidation replaced Mg in olivine and low-Ca pyroxene, in addition to converting some low-Ca pyroxene to olivine. The displaced Mg was presumably accommodated by changing the Ol/Px ratio proportionally. Although these observations appear to support oxidation during progressive metamorphism of ordinary chondrites, all these mineralogic trends are subtle and have only been documented in data averaged over each petrologic type (McSween and Labotka, 1993). Moreover, systematic changes in the modal (as opposed to normative) Ol/Px ratio in chondrites of different petrologic type have never been demonstrated, because of difficulties in optically point-counting chondrite sections.

There is also a substantial body of literature that postulates reduction, rather than oxidation, accompanied ordinary chondrite metamorphism. Measurements by Dodd (1976) and Sears and Weeks (1986) suggested that the abundance of total iron in ordinary chondrites increases with petrologic type, and these authors inferred that this trend reflected increases in metallic iron. However, analyses of metallic iron in ordinary chondrites by Jarosewich (1990) show the opposite trend. The contradiction between these observations may result from differences in the methods used to obtain metal abundances. Jarosewich (1990) physically separated metal, whereas Sears and Weeks (1986) inferred metal abundances from concentrations of other siderophile elements in bulk meteorite samples. Morgan *et al.* (1985) likewise used siderophile element concentrations to infer metal abundances, but their data indicate decreasing metal concentrations with increasing petrologic type. Brett and Sato (1984) measured intrinsic oxygen fugacities for ordinary chondrites using a solid-electrolyte oxygen cell. They found that the metamorphosed chondrites were more reduced than unmetamorphosed chondrites of the same class. Because bulk carbon content decreases with petrologic type, Brett and Sato (1984) attributed reduction to a reaction with graphite.

Here we critically evaluate hypotheses that chondrites were oxidized or reduced during metamorphism by measuring modal Ol/Px ratios in individual, metamorphosed L and LL chondrites. These data are compared to the normative Ol/Px ratios and to Ol/Px ratios calculated from VISNIR spectra of the same meteorites. We also examine Ni/Fe and Co/Fe in bulk metal and Fe/Mn and Fe/Mg systematics in silicates as indications of redox state.

METHODS

Three thin sections of L chondrites and five thin sections of LL chondrites, spanning petrologic types 4, 5, and 6, were examined (Table 1). Desirable characteristics for these chondrites included limited shock effects and lack of brecciation (Table 1). Olivenza (LL5) is characterized as a fragmental breccia, although the two sections used in this study did not contain recognizable clasts. All samples except Greenwell Springs (LL4) and Tuxtuac (LL5) were previously identified as "spectrally clean" by Gaffey (1999), indicating these meteorites are not contaminated with terrestrial weathering products. Iron oxides, in particular, create spectral effects that limit the

TABLE 1. L and LL ordinary chondrites examined in this study.

Chondrite classification	Name	Spectrally clean*	Shock grade	Sources†	Collection
L4	Bald Mountain	Y	S4	(3)	USNM 851-1
L5	Homestead	Y	S3	(3)	USNM 423
L6	Girgenti	Y	S4	(1)	USNM 1453-1
LL4	Greenwell Springs		S3	(1)	USNM 6379-2
LL5	Olivenza (1)	Y	S3‡	(2)	USNM 5955-1
LL5	Olivenza (2)	Y	S3‡	(2)	H. McSween
LL5	Tuxtuac		S2	(4)	Field ME 2850 No. 4
LL6	Saint-Sévérin	Y	S3	(1)	USNM 2608-3

*Gaffey (1999).

†Sources for shock classification: (1) this work, (2) Stöffler *et al.* (1991), (3) Rubin (1993), (4) Graham *et al.* (1985).

‡Fragmental breccia.

usefulness of weathered chondrites for calibration of asteroid spectra. However, terrestrial weathering of metal does not affect Ol/Px ratios, and thus does not interfere with testing hypotheses of oxidation *vs.* reduction during chondrite metamorphism. In any case, no spectra are available for Greenwell Springs and Tuxtuac.

Modal Mineralogy

Despite extensive studies of ordinary chondrites, modal mineralogy data sets have not been obtained. Chondrites tend to be fine grained, and optical discrimination of silicate phases is usually difficult. Electron microprobe compositional mapping provides an alternative to the traditional point-counting method. Modal abundances of minerals using the Feature Scan microanalysis technique were obtained with an Oxford Instruments (LINK) Model eXL II energy dispersive spectrometer (EDS) mounted on a Cameca SX-50 electron microprobe at the University of Tennessee. Preliminary analyses, using EDS, determined the major elements in the various phases of interest. Feature Scan allows user-defined windows to identify the phases present in a sample (Taylor *et al.*, 1996). For example, specific ranges of Si, Ca, and Mg contents were used to identify olivine. Table 2 lists the x-ray spectral criteria used to classify the various mineral and glass (silica) phases in these chondrites. Conditions were set for excitation potential of 20 kV, beam current of 3 nA, dwell (counting) time of 40–60 s, and beam size of ~1 μm.

Feature Scan has an estimated precision of ~5% of the amount of each mineral present (Taylor *et al.*, 1996). An EDS spectrum was acquired at every fourth pixel (step size ~16 μm). The number of points analyzed varied from ~10 000 to ~80 000 per thin section, significantly more than in conventional point-counting methods. EDS spectra that did not meet any defined mineral criteria (usually representing grain boundaries and unidentified minor phases) were unclassified. All mineral proportions were normalized to 100% after the unclassified points (average ~8% in each meteorite) were subtracted from the total (equivalent to distributing the unclassified points proportionally among each phase present). Proportional assignment of unclassified points that arise from grain boundaries is strictly correct only if the various minerals have the same grain size distribution. In this study, we focus only on olivines and pyroxenes, and calculated Ol/Px ratios with and without reassigned unclassified points are compared in Table 3. There is virtually no difference in these values, indicating that the incorrect assignment of unclassified points because of grain size effects is not a source of error in these data.

The modes that Feature Scan produces are given as percent of surface area, assumed to equal volume percent. In comparing the measured (modal) and normative mineral abundances, it is necessary to convert modal abundance to weight percent using the density of each phase (described in detail by Gastineau, 2000). Modal data, recast into weight percent, are presented in Table 3.

The modal abundances of kamacite and taenite (Table 3) are apparently inaccurate, because thin section areas are not representative for irregularly distributed metal grains (McSween *et al.*, 1991). Metal abundances, as well as average metal compositions, are more accurately determined from bulk chemical analyses, and data from Jarosewich (1990) are given in Table 4.

TABLE 2. X-ray spectral criteria used to classify minerals and glass phases.*

Phase†	Defining criteria‡
olivine	36–55% *Si*, 18–55% *Mg*, and 0–2% *Ca*
orthopyroxene	55–70% *Si*, 13–30% *Mg*, and 0–3% *Ca*
plagioclase	50–75% *Si* and 12–35% *Al*
diopside	45–70% *Si*, 5–20% *Mg*, 15–35% *Ca*, and 0–4% *Al*
pigeonite	55–70% *Si*, 12–25% *Mg*, and 3–12% *Ca*
troilite	>20% *S*
taenite	55–90% *Fe* and >20% *Ni*
kamacite	>80% *Fe* and >10% *Ni*
chromite	>20% *Cr*
ilmenite	>40% *Ti*
whitlockite	>10% *P* and >20% *Ca*
K-rich glass	>5% *K*
silica phase	38–66% *Si* and 4–15% *Al*

*These criteria are only applicable to identify phases in the L and LL meteorites of this study.

†The minerals and glasses are arranged according to a first fit. For example, if the EDS spectrum acquired for an analyzed phase does not meet the olivine criteria, Feature Scan then tests it for low-Ca pyroxene, *etc.*

‡These criteria are in terms of percentage of spectrum as provided by the Feature Scan x-ray imaging software. The values are similar to the oxide weight percentages for given elements.

Quantitative Chemical Analyses

Major and minor element compositions were determined by electron microprobe using the Cameca SX-50. The accelerating voltage was 15 kV with a beam current of 30 nA. A beam size of 1 μm and counting times of 20 s were used for all elements. All data were corrected using ZAF procedures incorporated in the Cameca software.

Analyses were obtained for four individual grains each of olivine, low-Ca pyroxene, and diopside in chondrites of petrologic types 5 and 6. Four grains of olivine and diopside and seven grains of low-Ca pyroxene were analyzed in meteorites of petrologic type 4. A minimum of two core and rim analyses were analyzed for each grain, although in some cases more analyses were obtained. Average analyses are presented for olivine, low-Ca pyroxene, and diopside in Tables 5, 6, and 7, respectively.

TABLE 3. Modal abundances for L and LL chondrites.

Phase	Meteorite							
	Bald Mountain (L4)	Homestead (L5)	Girgenti (L6)	Greenwell Springs (LL4)	Olivenza (LL5) (section 1)	Olivenza (LL5) (section 2)	Tuxtuac (LL5)	Saint-Sévérin (LL6)
olivine	34.2	35.0	41.6	43.1	50.2	49.3	48.3	52.2
orthopyroxene	27.0	26.8	26.1	23.0	19.3	21.3	19.2	20.9
pigeonite	6.81	3.92	1.68	4.96	2.93	1.76	2.59	1.61
diopside	1.95	2.19	5.15	2.66	3.91	3.33	4.70	5.47
plagioclase	5.66	6.45	9.55	7.83	10.01	10.87	9.23	10.50
silica phase	5.74	5.47	n.a.	6.65	4.69	3.01	3.92	n.a.
K-rich glass	0.06	0.04	n.a.	0.29	0.17	0.13	0.20	n.a.
whitlockite	0.60	0.41	0.58	0.73	0.75	0.47	0.42	0.34
ilmenite	0.00	0.00	0.00	0.00	0.00	0.01	0.05	0.00
chromite	0.67	0.73	1.00	0.91	1.15	0.81	1.01	1.06
kamacite	7.64	11.01	4.00	0.73	0.10	0.24	0.10	0.56
taenite	1.58	1.44	2.03	1.52	1.68	3.23	2.59	1.26
troilite	8.08	6.56	8.36	7.67	5.16	5.62	7.65	6.16
Total	100	100	100	100	100	100	100	100
Ol/Px*	1.01	1.14	1.50	1.54	2.26	2.14	2.22	2.32
Ol/Opx†	1.27	1.31	1.59	1.87	2.60	2.31	2.52	2.50
Ol/Px‡	1.01	1.14	1.50	1.54	2.26	2.14	2.22	2.32

n.a. = not analyzed.
*Px = orthopyroxene + pigeonite (unclassified points assigned to minerals).
†Opx = orthopyroxene (unclassified points assigned to minerals).
‡Px = orthopyroxene + pigeonite (without unclassified points).

TABLE 4. Bulk metal abundances and compositions.

Chondrite	Bulk metal abundance*	Ni/Fe	Co/Fe	Modal metal abundance†
Bald Mountain (L4)	8.44	0.149	0.0083	9.22
Homestead (L5)	8.05	0.163	0.0087	12.65
Girgenti (L6)	6.80	0.172	0.0103	6.03
Greenwell Springs (LL4)	3.12	0.346	0.0160	2.25
Olivenza (LL5)	1.54	0.883	0.0325	1.78/3.47‡
Tuxtuac (LL5)	n.a.	n.a.	n.a.	2.69
Saint-Sévérin (LL6)	2.15	0.488	0.0186	1.82

n.a. = not analyzed.
*Bulk metal abundances are from Jarosewich (1990).
†Modal metal abundances are the sum of kamacite and taenite from Table 3.
‡The separate values represent the two thin sections of Olivenza.

Spectral Reflectance Measurements

Reflectance spectra of chondrites were measured with a Beckman DK2A ratio recording spectroreflectometer equiped with an integrating sphere. The samples (except for Saint-Sévérin) were measured as unsorted particle size powders. The spectrum of Saint-Sévérin was measured on the broken surface of a chip. Details of the measurements are given by Gaffey (1976).

Band I (1 μm) and band II (2 μm) center positions and band II/band I area ratios (BAR) for spectrally analyzed chondrites are given in Table 8. The relative proportions of olivine and low-Ca pyroxenes, expressed as Px/(Ol + Px), are obtained using the following equation derived from Cloutis *et al.* (1986): $Px/(Ol + Px) = (0.417 \times BAR) + 0.052$. These mineral proportions have also been recalculated as Ol/Px for comparison with modal data (Table 8).

TABLE 5. Average electron microprobe analyses for olivine of each L and LL chondrites.

	G(L6) (16)*	H(L5) (16)	BM(L4) (24)	SS(LL6) (16)	O(LL5) (32)	T(LL5) (16)	GS(LL4) (24)
SiO_2	38.3 (1)†	37.9 (2)	38.2 (2)	37.6 (6)	37.1 (2)	37.2 (1)	36.8 (2)
TiO_2	<0.03	<0.03	<0.03	<0.03	<0.03	<0.03	<0.03
Al_2O_3	<0.03	<0.03	<0.03	<0.03	<0.03	<0.03	<0.03
Cr_2O_3	<0.03	<0.03	<0.03	0.03 (2)	0.03 (2)	0.03 (2)	<0.03
MgO	38.9 (2)	39.5 (2)	40.1 (1)	35.5 (1)	35.2 (1)	35.0 (0)	36.5 (1)
CaO	<0.03	0.03 (0)	<0.03	0.04 (1)	0.04 (1)	<0.03	<0.03
MnO	0.44 (1)	0.45 (2)	0.46 (2)	0.44 (1)	0.44 (2)	0.44 (0)	0.46 (2)
FeO	22.9 (0)	21.5 (9)	21.2 (1)	26.1 (3)	26.8 (2)	27.5 (2)	25.6 (1)
Na_2O	<0.03	<0.03	<0.03	<0.03	<0.03	<0.03	<0.03
Total	100.50	99.40	99.98	99.71	99.67	100.22	99.37
Cations based on four oxygens							
Si	0.994	0.989	0.990	1.000	0.993	0.991	0.982
Ti	0.000	0.000	0.000	0.000	0.000	0.001	0.000
Al	0.000	0.000	0.000	0.000	0.001	0.000	0.000
Cr	0.000	0.000	0.001	0.001	0.001	0.001	0.000
Mg	1.505	1.538	1.548	1.407	1.403	1.392	1.454
Ca	0.000	0.001	0.001	0.001	0.001	0.001	0.001
Mn	0.010	0.010	0.010	0.010	0.010	0.010	0.010
Fe	0.496	0.471	0.459	0.580	0.599	0.613	0.571
Na	0.000	0.000	0.001	0.000	0.001	0.000	0.000
Total	3.006	3.010	3.009	2.999	3.007	3.008	3.018
Fe/Mn	50.9	47.7	45.5	58.6	61.2	61.3	55.2
Fe/Mg	0.33	0.31	0.30	0.41	0.43	0.44	0.39

Abbreviations: G = Girgenti, H = Homestead, BM = Bald Mountain, SS = Saint-Sévérin, O = Olivenza, T = Tuxtuac, and GS = Greenwell Springs

*The number of analyses averaged.

†The number in parentheses represents the 1σ precision of replicate analyses as expressed by the least digit cited.

RESULTS

Modal Mineral Abundances

Modal Ol/Px ratios for the L and LL chondrites in this study are compared to normative Ol/Px ratios for the same meteorites in Fig. 1 and Table 8. For this calculation, modal Px is the sum of orthopyroxene and pigeonite (*i.e.*, low-Ca pyroxenes) in Table 3. The norm calculates only orthopyroxene (hypersthene); pigeonite is calculated as a mixture of hypersthene and diopside in the norm, but the amount of diopside is minor. For comparison purposes, we also include modal Ol/Opx ratios (*i.e.*, orthopyroxene without pigeonite) in Table 3; although modal Ol/Opx provides a closer match to normative Ol/Px, we do not believe that use of this ratio is justified in comparing with normative data, although it may be useful in comparison with spectrally derived Ol/Px.

The normative Ol/Px ratio increases with petrologic type in these L and LL chondrites, as it does in average L and LL chondrite data (McSween and Labotka, 1993). The modal Ol/Px ratio for the L chondrites likewise increases with petrologic type; however, each modal Ol/Px ratio is consistently offset to a lower value than the normative ratio for the same meteorite. The modal Ol/Px ratio for the LL chondrites also increases with petrologic type and is lower compared to the normative ratio, although its offset value for the LL5 chondrites is less than for other samples. The LL5 modal data include two different sections of Olivenza and one section of Tuxtuac, all of which have similar Ol/Px ratios; the LL5 normative ratio is for Olivenza only. The increasing Ol/Px ratios with petrologic type seen in both modal and normative data for individual chondrites support the hypothesis of oxidation, and are inconsistent with reduction.

Comparison of modal and normative mineralogies reveals several other interesting features. The modal abundances of diopside and plagioclase in L (Fig. 2a,b) and LL (Fig. 2c,d) chondrites increase with petrologic type (with the exception of plagioclase in Tuxtuac LL5). The modal and normative abundances of these two phases disagree in lower petrologic types, but converge in type 6 chondrites. Modal mineralogy also revealed a silica-rich phase, possibly glass (4–6 wt%); however, it was not discovered until after both type 6 chondrites had been analyzed. Therefore, it is not known if the silica phase may increase or decrease with petrologic type. The silica phase occurs within mesostasis material, texturally intergrown with plagioclase (Fig. 3) in most chondrites. This phase has

TABLE 6. Average electron microprobe analyses for low-Ca pyroxene of each L and LL chondrite.

	G(L6) (23)*	H(L5) (16)	BM(L4) (48)	SS(LL6) (16)	O(LL5) (32)	T(LL5) (16)	GS(LL4) (42)
SiO_2	55.3 (3)†	55.2 (4)	55.9 (2)	55.1 (1)	54.5 (2)	54.7 (1)	54.9 (3)
TiO_2	0.19 (3)	0.13 (4)	0.12 (5)	0.20 (3)	0.15 (4)	0.14 (3)	0.11 (3)
Al_2O_3	0.16 (2)	0.23 (21)	0.15 (7)	0.17 (1)	0.18 (12)	0.11 (2)	0.20 (9)
Cr_2O_3	0.12 (1)	0.19 (13)	0.12 (5)	0.15 (5)	0.14 (8)	0.07 (2)	0.17 (12)
MgO	29.1 (2)	29.5 (4)	30.0 (2)	27.2 (1)	27.3 (1)	27.2 (1)	28.0 (3)
CaO	0.81 (5)	0.65 (28)	0.43 (17)	0.88 (4)	0.80 (7)	0.72 (3)	0.51 (14)
MnO	0.47 (2)	0.46 (3)	0.46 (1)	0.44 (1)	0.44 (1)	0.45 (1)	0.44 (3)
FeO	13.9 (1)	13.3 (2)	13.0 (1)	15.8 (1)	15.8 (2)	16.4 (10)	15.4 (2)
Na_2O	<0.03	<0.03	<0.03	<0.03	<0.03	<0.03	<0.03
Total	99.99	99.67	100.23	99.94	99.32	99.78	99.67
Cations based on four oxygens							
Si	1.980	1.978	1.987	1.992	1.983	1.985	1.984
Ti	0.005	0.003	0.003	0.005	0.004	0.004	0.003
Al	0.006	0.010	0.006	0.007	0.008	0.004	0.008
Cr	0.003	0.012	0.004	0.004	0.004	0.002	0.005
Mg	1.552	1.575	1.587	1.463	1.482	1.474	1.508
Ca	0.031	0.025	0.016	0.034	0.031	0.028	0.020
Mn	0.014	0.014	0.014	0.013	0.013	0.014	0.013
Fe	0.417	0.399	0.387	0.477	0.481	0.497	0.465
Na	0.001	0.001	0.001	0.001	0.002	0.001	0.001
Total	4.010	4.011	4.005	3.998	4.008	4.008	4.007
Fe/Mn	29.2	28.7	28.1	35.4	35.9	35.8	34.6
Fe/Mg	0.27	0.25	0.24	0.33	0.32	0.34	0.31
Wo/Fs	1.6/20.9	1.3/20.0	0.8/19.4	1.7/24.2	1.6/24.1	1.4/24.9	1.0/23.3

Abbreviations: G = Girgenti, H = Homestead, BM = Bald Mountain, SS = Saint-Sévérin, O = Olivenza, T = Tuxtuac, and GS = Greenwell Springs.
*The number of analyses averaged.
†The number in parentheses represents the 1σ precision of replicate analyses as expressed by the least digit cited.

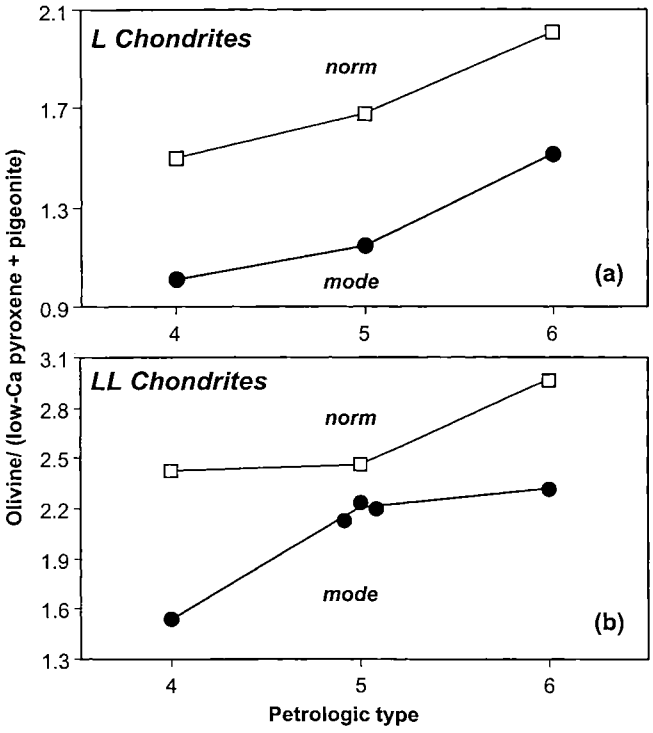

not been noticed or described in previous literature for types 5 and 6 chondrites. Unfortunately, our samples were too fine grained for microprobe characterization.

Olivine/Pyroxene Ratios from Spectra

The Ol/Px ratios calculated from reflectance spectra of L and LL chondrites (Table 8) also increase systematically with petrologic type. The spectrally derived Ol/Px for Bald Mountain (L4) agrees with the measured ratio, but Ol/Px ratios for the L5 and L6 chondrites deviate progressively from the measured ratios. No spectrally clean LL4 chondrites have been analyzed, but the LL5 and LL6 chondrites show the same kind of disagreement between spectrally derived and measured Ol/Px ratios. The algorithm used to calculate mineral proportions from reflectance spectra apparently systematically overestimates the Ol/Px ratios for L and LL chondrites of higher petrologic type. Nevertheless, the trends support oxidation rather than reduction during metamorphism.

FIG. 1. Both normative and modal Ol/Px ratios increase with petrologic type in (a) L and (b) LL chondrites. However, for each meteorite, the modal Ol/Px ratio is consistently lower than the normative ratio. Normative ratios were calculated by McSween *et al.* (1991), and modal ratios are based on data in Table 3.

TABLE 7. Average electron microprobe analyses for diopside of each L and LL chondrite.

	G(L6) (23)*	H(L5) (13)	BM(L4) (17)	SS(LL6) (24)	O(LL5) (16)	T(LL5) (16)	GS(LL4) (17)
SiO_2	53.9 (1)†	53.8 (2)	53.9 (3)	53.2 (2)	53.6 (3)	53.7 (1)	53.2 (3)
TiO_2	0.46 (1)	0.29 (9)	0.33 (5)	0.43 (1)	0.38 (5)	0.35 (2)	0.41 (8)
Al_2O_3	0.49 (2)	0.46 (3)	0.53 (15)	0.49 (1)	0.47 (4)	0.40 (2)	0.97 (30)
Cr_2O_3	0.79 (6)	0.80 (4)	1.18 (44)	0.78 (2)	0.70 (3)	0.69 (4)	0.97 (20)
MgO	16.7 (2)	16.8 (2)	17.6 (7)	16.1 (2)	16.4 (3)	16.2 (1)	16.9 (2)
CaO	21.7 (3)	22.1 (3)	20.1 (26)	21.4 (2)	21.4 (2)	22.0 (2)	20.4 (1)
MnO	0.23 (1)	0.20 (2)	0.30 (9)	0.23 (1)	0.22 (1)	0.20 (2)	0.24 (3)
FeO	4.79 (11)	4.19 (12)	4.80 (1.1)	6.03 (29)	5.65 (7)	5.56 (26)	5.53 (21)
Na_2O	0.54 (2)	0.56 (3)	0.65 (11)	0.51 (2)	0.49 (1)	0.46 (2)	0.50 (4)
Total	99.66	99.24	99.36	99.13	99.29	99.55	99.12
Cations based on four oxygens							
Si	1.982	1.983	1.978	1.977	1.983	1.984	1.967
Ti	0.013	0.008	0.009	0.012	0.011	0.010	0.011
Al	0.021	0.020	0.023	0.021	0.021	0.018	0.042
Cr	0.023	0.024	0.034	0.023	0.020	0.020	0.028
Mg	0.915	0.923	0.967	0.890	0.903	0.892	0.931
Ca	0.857	0.874	0.793	0.852	0.850	0.870	0.809
Mn	0.007	0.006	0.009	0.007	0.007	0.006	0.008
Fe	0.147	0.129	0.148	0.187	0.175	0.172	0.171
Na	0.038	0.040	0.046	0.037	0.035	0.033	0.036
Total	4.002	4.007	4.007	4.007	4.004	4.004	4.004
Fe/Mn	20.4	20.5	15.9	26.6	26.1	28.3	22.5
Fe/Mg	0.16	0.14	0.15	0.21	0.19	0.19	0.18
Wo/Fs	44.7/7.7	45.4/6.7	41.6/7.8	44.2/9.7	44.1/9.1	45.0/8.9	42.3/8.9

Abbreviations: G = Girgenti, H = Homestead, BM = Bald Mountain, SS = Saint-Sévérin, O = Olivenza, T = Tuxtuac, and GS = Greenwell Springs.

*The number of analyses averaged.

†The number in parentheses represents the 1σ precision of replicate analyses as expressed by the least digit cited.

TABLE 8. Spectral data for spectrally clean L and LL chondrites.

	Bald Mountain (L4)	Homestead (L5)	Girgenti (L6)	Olivenza (LL5)	Saint-Sévérin (LL6)
Band I*	0.93	0.945	0.958	1.015	0.980
Band II*	1.937	1.935	1.948	1.975	1.940
Band I/Band II area ratio (BAR)	0.897	0.831	0.552	0.388	0.308
Px/(Ol + Px)†	0.43	0.40	0.28	0.21	0.18
Spectra Ol/Px	1.33	1.50	2.57	3.76	4.56
Modal Ol/Px‡	1.01	1.14	1.50	2.26/2.14	2.32
Normative Ol/Px§	1.49	1.67	2.00	2.46	2.95

*Band I and II positions are in microns.

†Px/(Ol + Px) = (0.417 × BAR) + 0.052, derived from Cloutis *et al.* (1986).

‡Calculated from data in Table 3.

§McSween and Labotka (1993).

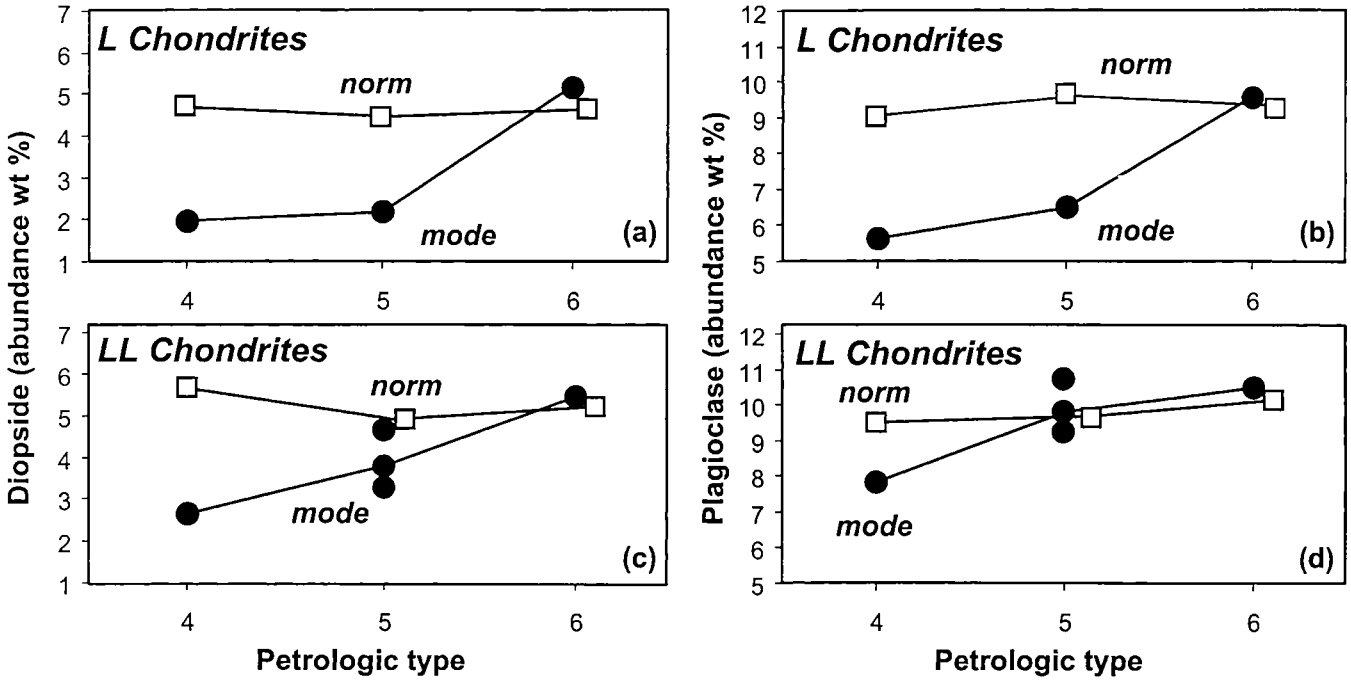

FIG. 2. Modal abundances of plagioclase and diopside increase with petrologic type in L (a, b) and LL (c, d) chondrites. Modal data (Table 3) are compared to normative mineral abundances for the same meteorites calculated by McSween *et al.* (1991).

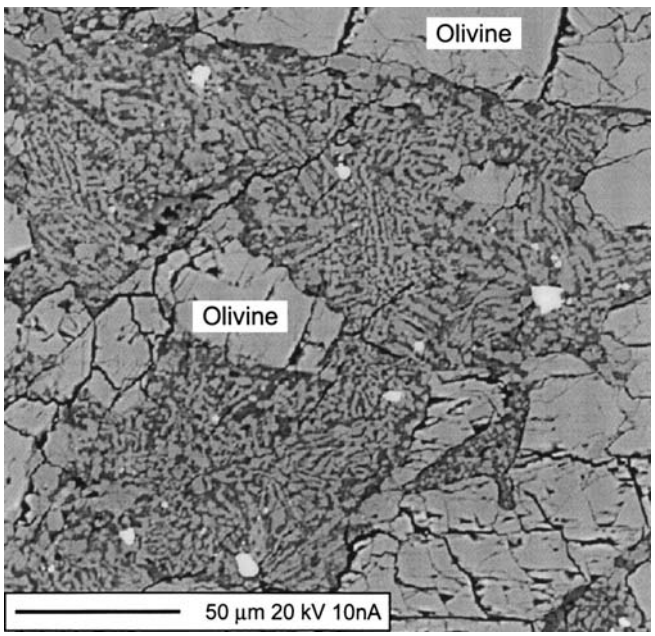

FIG. 3. Backscattered electron image of the Homestead L5 chondrite shows mesostasis material containing texturally intergrown plagioclase (light gray) and a high-silica phase (dark gray), coexisting with olivine.

Metal Abundances and Compositions

Bulk metal abundances of individual chondrites decrease with petrologic type for the L chondrites (Jarosewich, 1990), as seen in Table 4. This trend is unclear in the analyzed LL chondrites, although Saint Sévérin (LL6) contains less metal than Greenwell Springs (LL4). Ni/Fe and Co/Fe in bulk metal separates are also given in Table 4. These ratios for the L chondrites increase with petrologic type, but the LL5 chondrites again are out of sequence. Bulk metal decreases with petrologic type, coupled with increases in Ni/Fe and Co/Fe (also observed in average L and LL chondrite data by McSween and Labotka, 1993), are consistent with the oxidation hypothesis. Despite the apparent odd behavior of these LL5 chondrites, there is no evidence for reduction.

We also attempted to measure the chemical compositions of individual kamacite and taenite grains in these meteorites, but were frustrated because the metal was strongly zoned and contained intergrowths of plessite. However, analyses of kamacite by Rubin (1990) in many ordinary chondrites indicate that Ni/Fe and Co/Fe increase with petrologic type, supporting oxidation.

Variations in Olivine and Pyroxene Compositions

Using a plot of molar Fe/Mn and Fe/Mg ratios of bulk chondrites, Goodrich and Delaney (2000) reiterated the well-known redox relationships between the H, L, and LL chondrite classes. We have plotted the molar Fe/Mn and Fe/Mg ratios for olivine, low-Ca pyroxene, and diopside on the same diagram (analyzed L and LL chondrites, identified by solid symbols in Figs. 4 and 5, respectively, are labeled according to their petrologic type). Previously published electron microprobe data for these minerals in other L and LL chondrites have been plotted as open symbols (Figs. 4 and 5), and envelopes

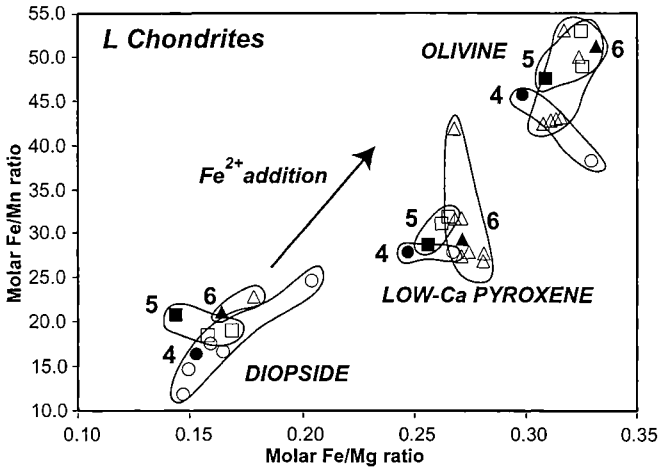

FIG. 4. Molar Fe/Mn and Fe/Mg ratios for silicate phases in L chondrites of different petrologic type, showing a general Fe enrichment trend in olivine and pyroxenes during metamorphism. Solid symbols present data collected in this study: circles for type 4, squares for type 5, and triangles for type 6. 1σ standard deviations in these data are smaller than the symbols. Envelopes enclose the molar ratios for olivine, low-Ca pyroxene, and diopside analyses (open symbols) in other L chondrites as described in the literature: Smith *et al.* (1972), Lange *et al.* (1973), Berkley *et al.* (1978), Keil *et al.* (1978), Dodd and Jarosewich (1981), Baryshnikova *et al.* (1985), Shervais *et al.* (1986), and Scorzelli *et al.* (1998).

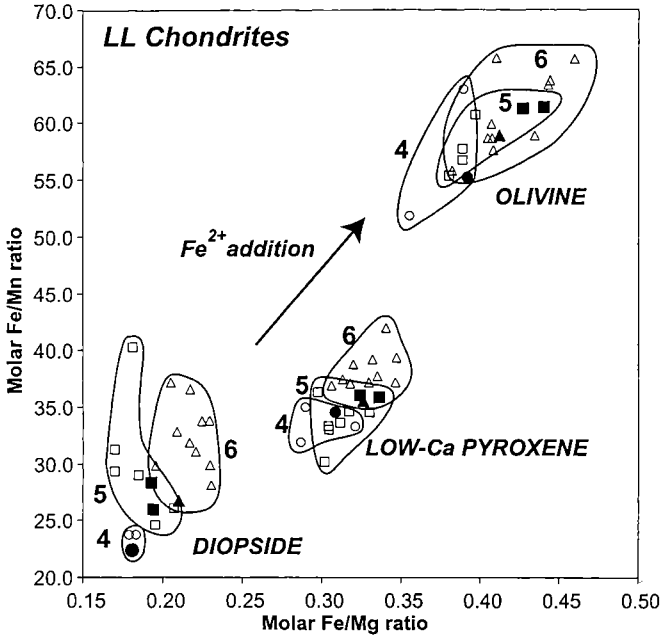

FIG. 5. Molar Fe/Mn and Fe/Mg ratios for silicate phases in LL chondrites of different petrologic type. Symbols are as in Fig. 4. Data sources for other LL chondrites: Heyse (1978), McSween and Patchen (1989), and Sighinolfi *et al.* (1991).

enclosing all these data illustrate the variability of Fe/Mn and Fe/Mg ratios for the different petrologic types. Arrows in these diagrams illustrate the expected effect of addition of Fe^{2+} produced by oxidation.

Data for different petrologic types show considerable overlap, but some trends can be discerned. For the L chondrites we studied (Fig. 4), molar Fe/Mn and Fe/Mg ratios for olivine and low-Ca pyroxene generally increase from petrologic types 4 to 6, although the data for diopside do not show a linear increase. For the LL chondrites we studied (Fig. 5), molar Fe/Mn and Fe/Mg ratios do not show systematic variations with petrologic type. When the overlapping envelopes enclosing all data in Figs. 4 and 5 are considered, petrologic types 4, 5, and 6 generally plot in an Fe-enrichment sequence; however, the data are too variable to constitute convincing evidence for or against oxidation.

Other elements in pyroxenes are also affected by metamorphism and behave identically in both L and LL chondrites. CaO content increases with petrologic type in low-Ca pyroxene (Table 6) and decreases in diopside (Table 7). This variation has already been well documented in pyroxenes of metamorphosed ordinary chondrites (Heyse, 1978; Brearley and Jones, 1998) and reflects attempts at equilibration between coexisting pyroxenes as a function of temperature (Lindsley, 1983). TiO_2 increases with petrologic type in low-Ca pyroxene (Table 6), as also noted by Komatsu and Miyamoto (1999), but TiO_2 concentration does not vary consistently in diopside (Table 7) (Brearley and Jones, 1998). Al_2O_3 and Cr_2O_3 do not vary consistently with petrologic type in either pyroxene. All minor oxides in olivine, with the exception of MnO, were at or below detection limits.

DISCUSSION

Comparison of Modal, Normative, and Spectrally Determined Olivine/Low-Calcium Pyroxene Ratios

Regardless of how they are determined, Ol/Px ratios increase with petrologic type, supporting the hypothesis that oxidation increases with progressive metamorphism in L and LL chondrites. We have found no evidence supporting the reduction hypothesis.

We do not understand the cause of the significant difference between modal and normative Ol/Px ratios. The greater proportion of olivine in the modal ratio reflects a higher silica content, relative to other oxides, than for the normative ratio. We doubt that unrepresentative sampling could account for such a consistent offset between modal and normative ratios. Jarosewich (1990), whose chemical analyses were the basis for the normative calculations, emphasized the importance of sample size in determining accurate abundances, and we are not aware of any systematic difference in Jarosewich's measured silica contents and those of other analysts. We recognize that the modest areas of thin sections may introduce some sample bias, but it is doubtful that offsets resulting from unrepresentative samples would be consistently in the same direction.

We also considered the possibility that the presence of a silica-rich phase (Fig. 3) might be responsible for the difference

between the modal and normative ratios. After all, a silica-saturated phase and magnesian olivine should not coexist at equilibrium, and they are not permitted to coexist in the normative calculation procedure. However, if this silica phase were responsible for the discrepancy, the modal Ol/Px ratio would be higher than normative Ol/Px (opposite to what is observed), because the normative uses the excess silica to produce more pyroxene at the expense of olivine.

The C.I.P.W. normative was designed to calculate the mineralogy of terrestrial igneous rocks, so it might be expected to have difficulty in dealing with reduced, metal-bearing rocks such as ordinary chondrites. McSween *et al.* (1991) noted that the Fe/Mg partitioning between normative olivine and low-Ca pyroxene disagrees with actual measured mineral partitioning in chondrites and in experimental charges (Madaris, 1969). It is not obvious how this failure to calculate the correct mineral compositions might relate to an incorrect calculation of the normative Ol/Px ratio. However, we are forced to conclude that the normative calculation may not provide an adequate estimation of the modal silicate mineralogy of ordinary chondrites, despite the widespread use of this method as the primary source of chondrite mineral abundances for half a century (*e.g.*, Wahl, 1951; Mason, 1965; Dodd, 1981; McSween *et al.*, 1991).

The cause of the discrepancy between modal (or normative) Ol/Px ratios and those calculated from spectra are also unknown, but may be related to spectral complexities introduced by other minerals. The spectral calibration is based on simple mixtures of olivine and low-Ca pyroxene (Cloutis *et al.*, 1986). The addition of a small amount of high-Ca pyroxene, as occurs in ordinary chondrites, can have significant spectral consequences. The presence of a second pyroxene is known to affect the band I center position, and band areas might also be affected. Ordinary chondrites actually contain three pyroxenes—orthopyroxene, diopside, and pigeonite—which may further complicate spectral interpretations. In any case, the differences between modal and spectral data appear to be systematic and repeatable, and hence correctable.

Mineral Disequilibrium

Some increases in the molar Fe/Mn and Fe/Mg ratios in olivine and pyroxenes with petrologic type (Figs. 4 and 5) may reflect oxidation during metamorphism. However, the observed overlaps in the envelopes for each petrologic type require comment. It is easy to forget that the boundaries between petrologic types are arbitrary breaks within a gradational sequence. Thus, chondrites assigned the same petrologic type may have experienced very different peak metamorphic temperatures, whereas the temperature differences for several chondrites assigned to different petrologic types might have been relatively small. For example, one type 5 chondrite may have been heated to a peak temperature close to the threshold for type 6, and another type 5 chondrite may have experienced a peak temperature only slightly above that for type 4.

In addition to increasing the Fe/Mn and Fe/Mg ratios of olivine, low-Ca pyroxene, and diopside, metamorphism also homogenized these phases by obliterating chemical zoning within grains and compositional differences between grains. Thus, we might expect that these phases were in equilibrium at the peak of metamorphism. Using the Fe/Mn *vs.* Fe/Mg diagram, tie-lines connecting olivine and diopside to low-Ca pyroxene in chondrites of the same petrologic type can be used to test whether these phases constitute an equilibrium assemblage. We expect that tie-lines joining the compositions of equilibrated minerals should either be parallel or change slopes systematically with petrologic type. The tie-lines connecting diopside, low-Ca pyroxene, and olivine based on our analyses and on literature data for L (Fig. 6) and LL (Fig. 7) chondrites often intersect. The preponderance of crossing tie-lines suggests that equilibrium either was not obtained at peak metamorphic conditions or was not maintained during cooling.

Erasure of zoning suggests that olivine, low-Ca pyroxene, and diopside may have reached equilibrium at peak metamorphic temperatures, but during cooling the diffusion of Fe, Mg, and Mn continued until different blocking temperatures were reached for each mineral. Fe/Mg diffusion in pyroxenes and olivine occurs at temperatures even lower than for Ca (Jurewicz and Watson, 1988). McSween and Patchen (1989) previously found evidence for disequilibrium in the CaO contents of coexisting low-Ca pyroxene and diopside in LL6 chondrites. They speculated that the coexisting pyroxenes in type 6 chondrites equilibrated during peak metamorphism, but differences in the degree of re-equilibration of the coexisting pyroxenes occurred on cooling. Variations in the slopes of the solvus limbs for low-Ca pyroxene and diopside (Lindsley, 1983) require a greater Ca compositional change in diopside with decreasing increments of temperature, relative to low-Ca pyroxene. If Ca diffusion occurred on cooling, we might also expect that Fe/Mg and Fe/Mn ratios would re-equilibrate.

Implications for Asteroid Spectroscopy

Three prominent spectral features in the VISNIR region are used to identify ferromagnesian mineral abundances and compositions on an asteroid surface: (1) band I center is controlled mostly by the Ca^{2+} content of pyroxene and the relative proportions of olivine and pyroxene (Adams, 1974), (2) band II center gives the pyroxene Fe^{2+} content (Adams, 1974), and (3) band II/band I area ratio is a function of the olivine/low-Ca pyroxene abundance ratio (Cloutis *et al.*, 1986). Figure 8a illustrates the spectral features of seven different S asteroid types (Gaffey *et al.*, 1993), each representing a portion of a continuous suite of silicate phases ranging from pure olivine (band II/band I = 0.0) to pure low-Ca pyroxene (2.8 > band II/band I > 1.6). The heavy line in Fig. 8a was defined by mixtures of olivine and pyroxene (Cloutis *et al.*, 1986).

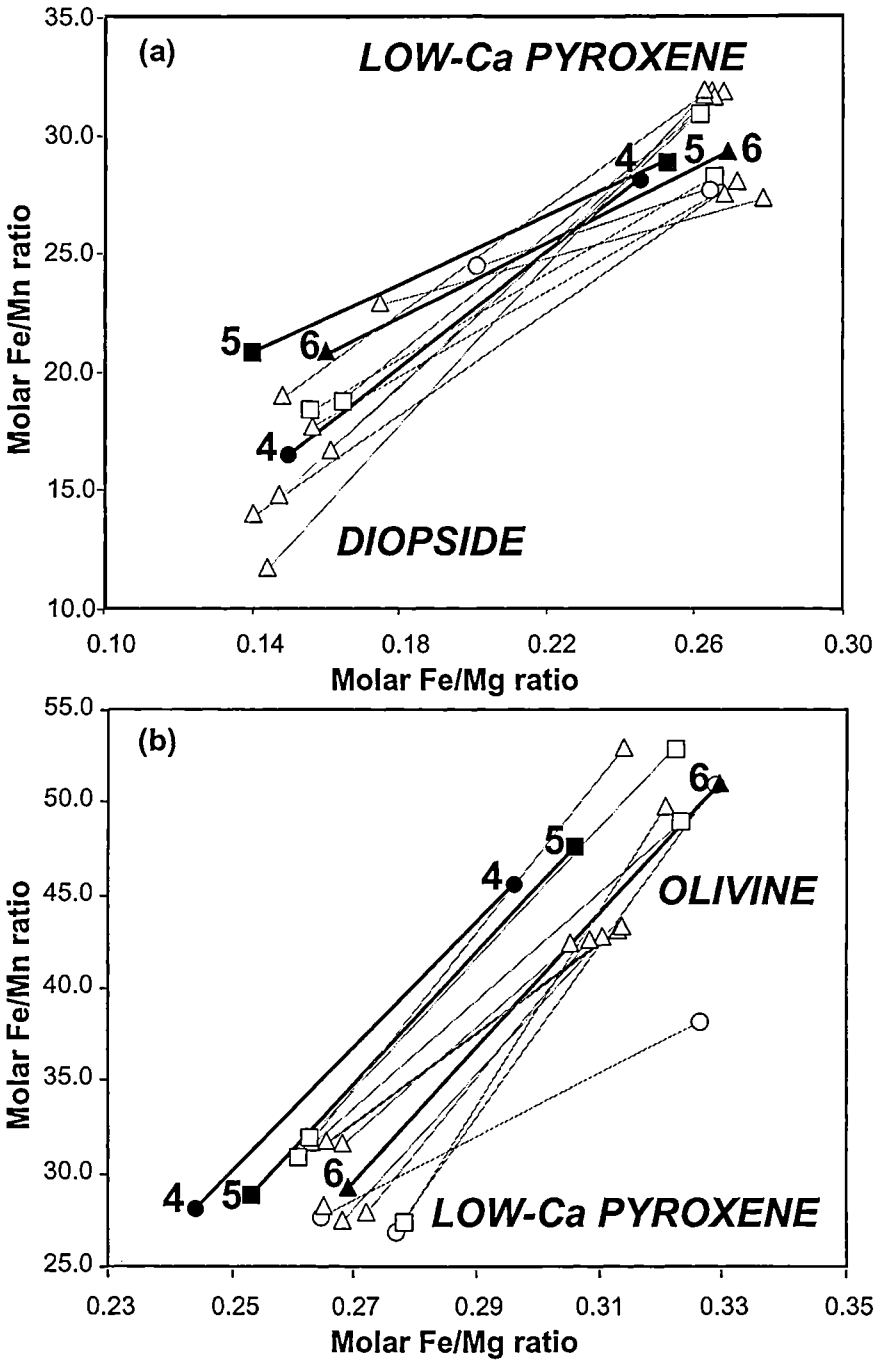

FIG. 6. Tie-lines connecting coexisting (a) low-Ca pyroxene and diopside, and (b) olivine and low-Ca pyroxene in L chondrites commonly intersect. Data from this study are shown as filled symbols connected by heavy tie-lines, and data from other sources (see Fig. 4) are shown as open symbols connected by dashed tie-lines.

S(IV) objects may have mineral assemblages spectrally similar to ordinary chondrites (Gaffey *et al.*, 1993; Murchie and Pieters, 1996). Gaffey and Gilbert (1998) compiled laboratory spectra, plotting in the S(IV) field, for L and LL chondrites of different petrologic types, shown by shaded areas in Fig. 8b. The spectrally clean L4, L5, and L6 chondrites in this study, also shown in Fig. 8b, plot in locations that reflect their increasing Ol/Px ratios. In terms of their band II/band I area ratios, which were used to estimate Ol/Px, the LL5 and LL6 chondrites show a similar trend (Fig. 8b). However, band I center also varies with Ol/Px (see the mixing line in Fig. 8a), and the positions of these meteorites are reversed for this parameter. Correcting for olivine content would shift the band I position for the LL chondrite spectra downward to the mixing line.

The utility of these spectral variations lies in their ability to define chondrite classes and petrologic types using Earth-

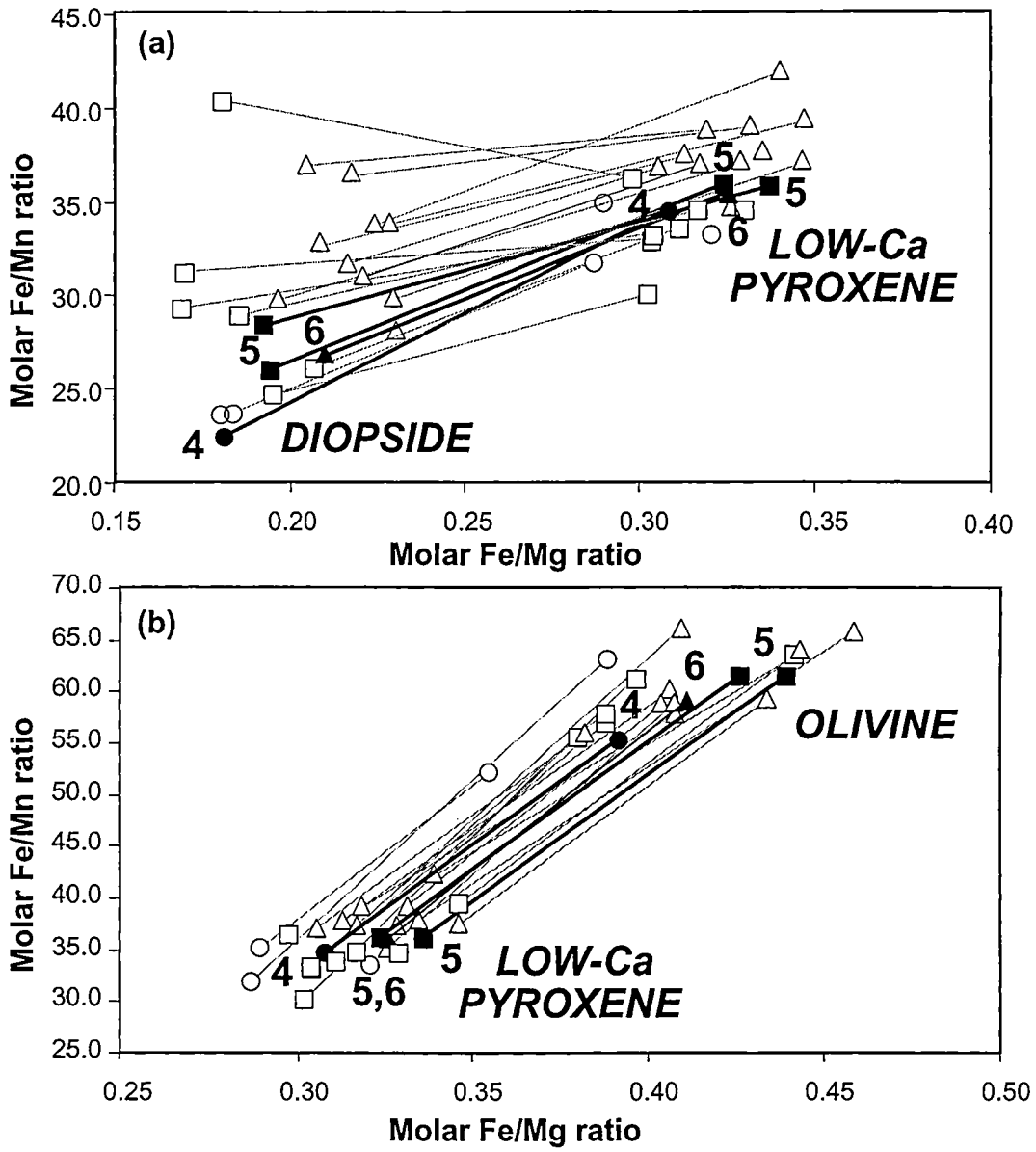

FIG. 7. Tie-lines connecting coexisting (a) low-Ca pyroxene and diopside, and (b) olivine and low-Ca pyroxene in LL chondrites also commonly intersect. Other data sources are given in Fig. 5.

based observations of asteroids. Variations in rotational spectra have been measured for a number of S asteroids (Gaffey, 1984; Gaffey and Ostro, 1987; Gaffey and Gilbert, 1998). Assuming that these asteroids have rubble-pile structures, materials of different metamorphic grade could plausibly be exposed on each asteroid surface. Changes in Ol/Px associated with oxidation during metamorphism may account for the observed spectral variations (McSween, 1992; Gaffey and Gilbert, 1998). Mineralogic interpretation of asteroid spectra may be complicated, however, by modest shifts of band positions at low temperatures in space (Singer and Roush, 1985; Moroz *et al.*, 2000).

Although the trends in spectrally determined Ol/Px ratios with petrologic type mimic the measured Ol/Px ratios, there are systematic differences in the absolute values of these ratios. The modal data presented here, and the normative data presented by McSween *et al.* (1991), will be used to calibrate empirically the relationship between ordinary chondrite phase abundances and the band II/band I area ratios in the spectra of such assemblages.

Orbital VISNIR spectra of asteroid 433 Eros have also been obtained by the *NEAR–Shoemaker* spacecraft. The average spectrum of Eros (Murchie and Pieters, 1996) plots within or slightly outside the S(IV) asteroid group. NEAR orbital spectra indicate a spectrally uniform surface similar to L and LL chondrites (Bell *et al.*, 2000; Veverka *et al.*, 2000). Once spectra collected in Eros orbit are properly calibrated, they may be mineralogically interpreted using the modal data presented

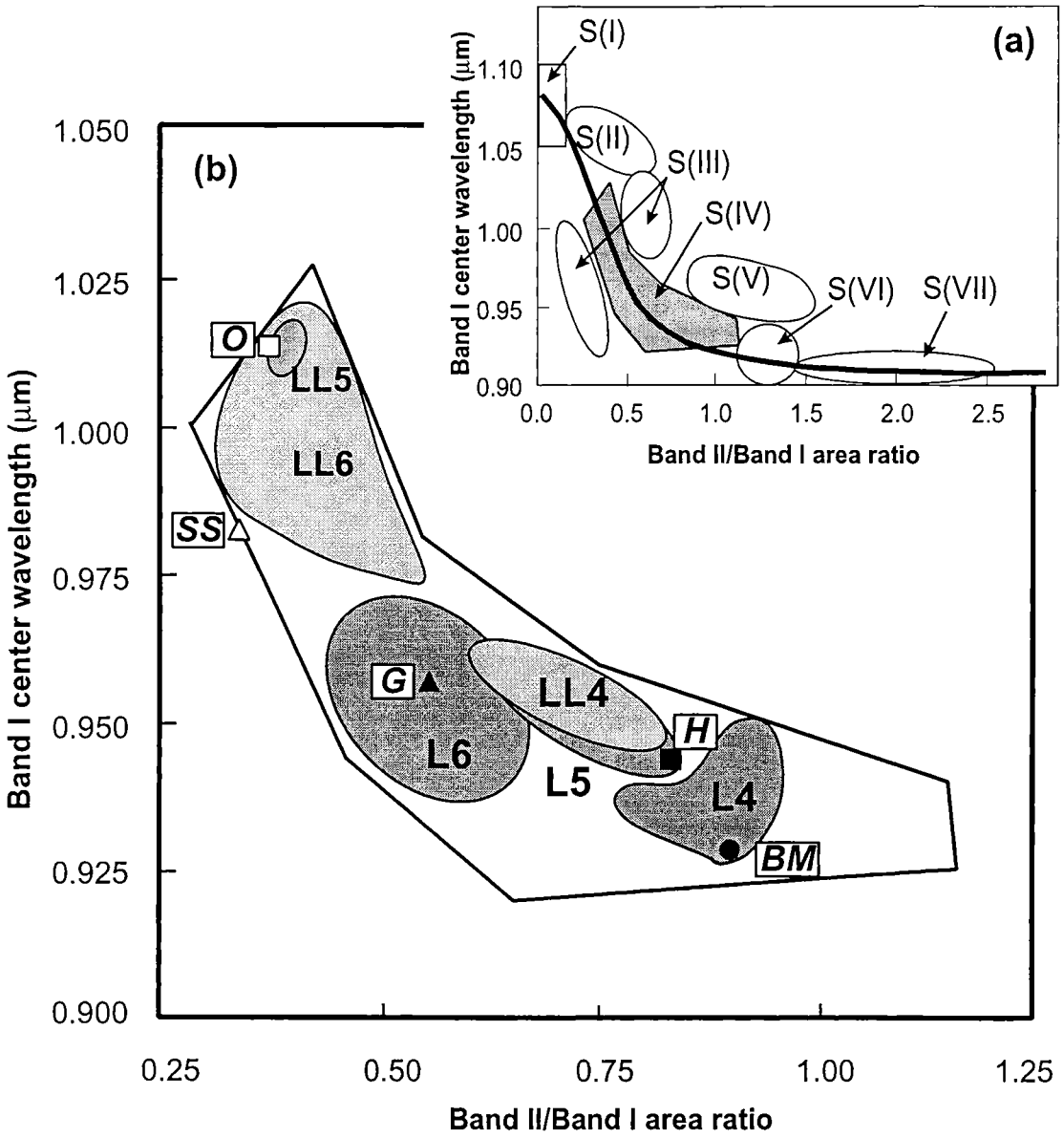

FIG. 8. Spectral features used to classify S asteroids and ordinary chondrites, modified from Gaffey *et al.* (1993) and Gaffey and Gilbert (1998). (a) Subdivision of S asteroids into seven spectral classes. The solid curve represents a simple mixing line between olivine at upper left and orthopyroxene at lower right (Cloutis *et al.*, 1986). S(IV) asteroids provide the closest spectral match to ordinary chondrites. (b) Expanded view of the outline of the S(IV) field, with areas enclosing the laboratory spectra of L4, L5, and L6 chondrites (dark gray) and LL4, LL5, and LL6 chondrites (shaded). Data for spectrally clean chondrites in this study (Table 8) are shown by symbol shapes as in Figs. 4 and 5 and abbreviated names as in Table 5.

here, to assess the relative fractions of chondrites of different metamorphic grades in producing the asteroid's regolith.

CONCLUSIONS

Modal Ol/Px ratios measured in individual L chondrites increase with petrologic type, supporting the hypothesis that oxidation occurred during metamorphism (McSween and Labotka, 1993). Metal abundances in these same chondrites decrease with petrologic type, and bulk metal Ni/Fe and Co/Fe ratios increase, also consistent with oxidation. Oxidation of metallic iron provided Fe^{2+} which transformed some low-Ca pyroxene into olivine. The trends for LL chondrites are not as clear, because LL5 chondrites (Olivinza and Tuxtuac) fall out of sequence. However, there is no evidence in the LL data for reduction during metamorphism.

Normative Ol/Px ratios are consistently higher than modal Ol/Px ratios for the same meteorites. Although we cannot yet explain this discrepancy, it suggests that the C.I.P.W. normative calculation procedure may not be appropriate for estimating mineral proportions in reduced, metal-bearing chondrites. Normative Ol/Px ratios and Ol/Px ratios calculated from

VISNIR spectra for these L and LL chondrites also increase with petrologic type. However, the spectrally determined Ol/Px ratios differ systematically from the modal and normative ratios for the same meteorites, possibly because of spectral complexities resulting from additional phases in chondrites such as diopside and pigeonite.

Many molar Fe/Mn and Fe/Mg ratios of olivine, low-Ca pyroxene, and diopside in our analyzed chondrites appear to increase with petrologic type, but the trends are indistinct. Nevertheless, we argue that they support some exchange of newly oxidized Fe^{2+} with residual minerals. Our analyses are consistent with previously published mineral data, which define partly overlapping fields for each petrologic type. Overlaps may result from the fact that the boundaries between petrologic types are breaks within a continuous metamorphic sequence, or failure to achieve or maintain equilibrium. Crossing tie-lines connecting the compositions of olivine, low-Ca pyroxene, and diopside indicate disequilibrium, probably due to varying degrees of re-equilibration of different minerals during cooling.

Characteristic VISNIR spectral absorption features are sensitive to the relative proportions and compositions of pyroxenes and olivine. This work documents that different petrologic types of L and LL chondrites have distinct Ol/Px ratios and pyroxene compositions acquired during metamorphism. These data should allow more accurate calibration of reflectance spectra for determining mineral abundances and compositions on the surfaces of chondritic asteroids using ground-based telescopes and the spectrometer aboard the *NEAR–Shoemaker* spacecraft.

Acknowledgments–Meteorite samples were provided by the Smithsonian Institution and the Field Museum of National History. We acknowledge the assistance of Allan Patchen in electron microprobe analyses, and particularly insightful reviews by Janice Bishop and Rhian Jones. This work was partly supported by NASA Cosmochemistry grant NAG-54541 to H. Y. M. and NASA Planetary Geology and Geophysics grant NAG5-10345 to M. J. G.

Editorial handling: S. R. Taylor

REFERENCES

ADAMS J. (1974) Visible and near-infrared diffuse reflectance spectra of pyroxenes as applied to remote sensing of solid objects in the solar system. *J. Geophys. Res.* **79**, 4829–4836.

BARYSHNIKOVA G. V., STAKHEYEVA S. A., IGNATENKO K. I. AND LAVRUKHINA A. K. (1985) Pyroxenes in H- and L-group ordinary chondrites. *Geochem. Intern.* **22**, 78–91.

BELL J. F., III *ET AL.* (2000) A search for small-scale spectral heterogeneity on 433 Eros from near-infrared spectrograph observations (abstract). *Meteorit. Planet. Sci.* **35 (Suppl.)**, A23.

BERKLEY J. L., KEIL K., GOMES C. B. AND CURVELLO W. S. (1978) Studies of Brazilian meteorites XII. Mineralogy and petrology of the Santa Bárbara, Rio Grande do Sul, chondrite. *An. Acad. Brasil Ciênc.* **50**, 191–196.

BREARLEY A. J. AND JONES R. H. (1998) Chondritic meteorites. In *Planetary Materials* (ed. J. J. Papike), pp. 3-1 to 3-398. Rev. Mineralogy **36**, Mineral. Soc. America, Washington, D.C., USA.

BRETT R. AND SATO M. (1984) Intrinsic oxygen fugacity measurements on seven chondrites, a pallasite, and a tektite and the redox state of meteorite parent bodies. *Geochim. Cosmochim. Acta* **48**, 111–120.

CLOUTIS E. A., GAFFEY M. J., JACKOWSKI T. L. AND REED K. L. (1986) Calibrations of phase abundance, composition and particle size distribution for olivine-orthopyroxene mixtures from reflectance spectra. *J. Geophys. Res.* **91**, 11 641–11 653.

DODD R. T. (1976) Iron-silicate fractionation within ordinary chondrite groups. *Earth Planet. Sci. Lett.* **28**, 479–484.

DODD R. T. (1981) *Meteorites: A Petrologic–Chemical Synthesis*. Cambridge Univ. Press, New York, New York, USA. 368 pp.

DODD R. T. AND JAROSEWICH E. (1981) Chemical variations among L-group chondrites, III. Major element variation in L6 chondrites. *Meteoritics* **16**, 93–111.

GAFFEY M. J. (1976) Spectral reflectance characteristics of the meteorite classes. *J. Geophys. Res.* **81**, 905–920.

GAFFEY M. J. (1984) Rotational spectral variations of asteroid (8) Flora: Implications for the nature of the S-type asteroids and for the parent bodies of the ordinary chondrites. *Icarus* **60**, 83–144.

GAFFEY M. J. (1999) Improving methodologies for quantitative interpretation of S(IV)/OC type: Asteroidal spectra with applications for the NEAR Eros mission (abstract). *Lunar Planet. Sci.* **30**, #1375, Lunar and Planetary Institute, Houston, Texas, USA (CD-ROM).

GAFFEY M. J. AND GILBERT S. L. (1998) Asteroid 6 Hebe: The probable parent body of the H-type ordinary chondrites and the IIE iron meteorites. *Meteorit. Planet. Sci.* **33**, 1281–1295.

GAFFEY M. J. AND OSTRO S. J. (1987) Surface lithologic heterogeneity and body shape for asteroid 15 Eunomia (abstract). *Lunar Planet. Sci.* **18**, 310–311.

GAFFEY M. J., BELL J. F., BROWN R. H., BURBINE T. H., PIATEK J. L., REED K. L. AND CHAKY D. A. (1993) Mineralogical variations within the S-type asteroid class. *Icarus* **106**, 573–602.

GASTINEAU H. K. (2000) A test for oxidation during metamorphism of L and LL chondrites. M. S. thesis, University of Tennessee, Knoxville, Tennessee, USA. 73 pp.

GOODRICH C. A. AND DELANEY J. S. (2000) Fe/Mg-Fe/Mn relations of meteorites and primary heterogeneity of primitive achondrite parent bodies. *Geochim. Cosmochim. Acta* **64**, 149–160.

GRAHAM A. L., BEVAN A. W. R. AND HUTCHISON R. (1985) *Catalogue of Meteorites*. Univ. Arizona Press, Tucson, Arizona, USA. 460 pp.

HEYSE J. V. (1978) The metamorphic history of LL-group ordinary chondrites. *Earth Planet. Sci. Lett.* **40**, 365–381.

JAROSEWICH E. (1990) Chemical analyses of meteorites: A compilation of stony and iron meteorite analyses. *Meteoritics* **25**, 323–337.

JUREWICZ A. J. G. AND WATSON E. B. (1988) Cations in olivine, Part 2: Diffusion in olivine xenocrysts, with applications to petrology and mineral physics. *Contrib. Mineral. Petrol.* **99**, 186–201.

KEIL K., LANGE D., ULBRICH M. N. C., GOMES C. B., JAROSEWICH E., ROISENBERG A. AND SOUZA M. J. (1978) Studies of Brazilian meteorites XIII. Mineralogy, petrology, and chemistry of the Putinga, Rio Grande do Sul, chondrite. *Meteoritics* **13**, 165–175.

KOMATSU M. AND MIYAMOTO M. (1999) Behavior of minor elements in olivine and orthopyroxene during metamorphism in LL chondrites (abstract). *Antarctic Meteorites* **24**, 85–87.

LANGE D. E., MOORE C. B. AND RHOTON K. (1973) The Willowbar meteorite. *Meteoritics* **8**, 201–256.

LINDSLEY D. H. (1983) Pyroxene thermometry. *Am. Mineral.* **68**, 477–493.

MADARIS G. (1969) Partitioning of Fe^{++} and Mg^{++} between coexisting synthetic olivine and orthopyroxene. *Am. J. Sci.* **267**, 945–968.

MASON B. (1965) The chemical composition of olivine-bronzite and olivine-hypersthene chondrites. *Am. Mus. Novitates* **2223**, 1–38.

MCSWEEN H. Y., JR. (1992) Redox effects in ordinary chondrites and implications for asteroid spectrophotometry. *Icarus* **95**, 239–243.

MCSWEEN H. Y., JR. AND LABOTKA T. C. (1993) Oxidation during metamorphism of the ordinary chondrites. *Geochim. Cosmochim. Acta* **57**, 1105–1114.

MCSWEEN H. Y., JR. AND PATCHEN A. D. (1989) Pyroxene thermobarometry in LL-group chondrites and implications for parent body metamorphism. *Meteoritics* **24**, 219–226.

MCSWEEN H. Y., JR., BENNETT M. E., III AND JAROSEWICH E. (1991) The mineralogy of ordinary chondrites and implications for asteroid spectrophotometry. *Icarus* **90**, 107–116.

MORGAN J. W., JANSSENS M. J., TAKAHASHI H., HERTOGEN J. AND ANDERS E. (1985) H-Chondrites: Trace element clues to their origin. *Geochim. Cosmochim. Acta* **49**, 247–259.

MOROZ L., SCHADE U. AND WASCH R. (2000) Reflectance spectra of olivine-orthopyroxene-bearing assemblages at decreased temperatues: Implications for remote sensing of asteroids. *Icarus* **147**, 79–93.

MURCHIE S. L. AND PIETERS C. M. (1996) Spectral properties and rotational spectral heterogeneity of 433 Eros. *J. Geophys. Res.* **101**, 2201–2214.

RUBIN A. E. (1990) Kamacite and olivine in ordinary chondrites: Intergroup and intragroup relationships. *Geochim. Cosmochim. Acta* **54**, 1217–1232.

RUBIN A. E. (1993) Metallic copper in ordinary chondrites. *Meteoritics* **29**, 94–98.

SEARS D. W. G. AND WEEKS K. S. (1986) Chemical and physical studies of type 3 chondrites, VI: Siderophile elements in ordinary chondrites. *Geochim. Cosmochim. Acta* **50**, 2815–2832.

SCORZELLI R. B., MICHEL-LÉVY M. C., GILABERT E., LAVIELLE B., AZEVEDO I. S., VIEIRA V. W., COSTA T. V. V. AND ARAÚJO M. A. B. (1998) The Campos Sales meteorite from Brazil: A lightly shocked L5 chondrite fall. *Meteorit. Planet. Sci.* **33**, 1335–1337.

SHERVAIS J. W., TAYLOR L. A., CIRLIN E., JAROSEWICH E. AND LAUL J. C. (1986) The Maryville meteorite: A 1983 Fall of an L6 chondrite. *Meteoritics* **21**, 33–45.

SIGHINOLFI G. P., GARUTI G. AND MORAIS E. (1991) The Jolomba, Angola, LL6 chondrite. *Meteoritics* **26**, 27–29.

SINGER R. B. AND ROUSH T. L. (1985) Effects of temperature on remotely sensed mineral absorption features. *J. Geophys. Res.* **90**, 12 434–12 444.

SMITH D. G. W., BELL J. D. AND FRISCH T. (1972) The Timersoi, Niger, hypersthene chondrite. *Meteoritics* **7**, 1–16.

STÖFFLER D., KEIL K. AND SCOTT E. R. D. (1991) Shock metamorphism of ordinary chondrites. *Geochim. Cosmochim. Acta* **55**, 3845–3867.

TAYLOR L. A., PATCHEN A., TAYLOR D. S. AND CHAMBERS J. G. (1996) X-ray digital imaging petrography of lunar mare soils: Modal analyses of minerals and glasses. *Icarus* **124**, 500–512.

VEVERKA J. *ET AL.* (2000) Near at Eros: Imaging and spectral results. *Science* **289**, 2088–2097.

WAHL W. (1951) The statement of chemical analyses of stony meteorites and the interpretation of the analyses in terms of minerals. *Mineral. Mag.* **29**, 416–426.